Journal of Engineering and Technology Research Vol.1 (8), pp.171-180, November, 2009
Available online at http://www.academicjournals.org/jetr
ISSN 2006-9790© 2009 Academic Journals

Full Length Research Paper

Combined low-Reynolds-number *k–ω* model with length scale correction term for recirculating flows

K. Khuwaranyu and S. Putivisutisak*

Mechanical Engineering Department, Chulalongkorn University,Patumwan, Bangkok, 10330, Thailand.

Accepted 26 October, 2009

A concept for a new turbulence model, which combines the Low-Reynolds-Number (LRN) *k–ω* model with a Length Scale Correction (LSC) term is proposed. The present model was developed for solving recirculating flow which is an important feature in many engineering applications. The LSC term employed here is *ω*–LSC – a new LSC uses the analogy of Yap correction. By integrating the term with the conventional LRN *k–ω* model, the turbulent length scale in the near-wall region is reduced which subsequently leads to better prediction of separations and reattachments that occur in this area. The developed model is validated with benchmark problems (the fully developed channel flow and backward-facing step flow) before being applied to the problem of recirculating flow over repeated square ribs. Performance of the model is investigated and compared with available experimental data, Direct Numerical Simulation (DNS) data and numerical results using other turbulence models. It is seen that the model gives superior results especially for the near-wall flow patterns.

Key words: Low-Reynolds-number *k–ω* model, recirculating flows, length scale correction, finite volume method and BLL model.

INTRODUCTION

Turbulence models are widely used for simulating complex heat transfer and flow phenomena in many engineering applications because of their simplicity and effectiveness. The most popular form is the one proposed by Launder and Spalding (1972), the so called the standard k–ε model (High-Reynolds model, High-Re). However, the disadvantage of the standard k–ε model with wall functions is the inability to predict accurate near-wall flow characteristics. The lack of universality of the wall functions has been frequently criticized. Inaccuracy and numerical stiffness may arise when the wall function is employed (Patel et al., 1985). To solve the near-wall effect, a number of Low-Reynolds-Number models (LRN model) have been developed (Peng and Davidson, 1997).

The first LRN k–ε model was developed by Jones and Launder (1973) and subsequently modified by many researchers. To get a better understanding of the near-wall effect, many LRN models were proposed by introducing the damping functions and other additional terms. Most of LRN models were developed based on the High-Re k–ε model (Lam and Bremhorst, 1981; Chien, 1982; Abe et al., 1994; Chang et al.,1995). However, the LRN models shared a weak point with the LRN k–ε model which was the uncertainty of ε specification at the wall (Peng and Davidson, 1997). In recent years, some new LRN two-equation models have been proposed as alternatives to the LRN k–ε models, e.g., the LRN k–τ model by Speziale et al. (1992) and the standard k–ω model and its LRN variant by Wilcox (1988, 1994).

The standard k–ω model was validated by a case of the boundary-layer and free shear flows. Patel and Yoon (1995) obtained accurate results using the standard k–ω model to solve separated flows over rough surfaces. Abid (1993) used the k–ω model in combination with an explicit algebraic stress model for recirculating flows, and obtained good agreement with the experiment. Larsson (1999) applied the k–ω model to predict the turbine blade heat transfer and concluded that the k–ω model performed as well as the k–ε model. Peng et al. (1997) modified the damping functions, the model constants of Wilcox's LRN k–ω model, and separated specific dissipation rate (ω) into two parts. After that, Peng and Davidson (1999) implemented the LRN k–ω model (Abid, 1993) by introducing a damping function into the turbulent kinetic energy term. Their model was compared with two LRN k–ε models and one LRN k–ω model.

*Corresponding author. E-mail: sompong.pu@chula.ac.th.

Several concepts were also used to increase model accuracy. Menter (1992) proposed a model to resolve the free-stream dependency by blending the standard Wilcox model and the standard *k–ε* model (in a *k–ω* formulation). Combining the High-Re *k–ω* model with the *k–ε* model, Menter (1994) developed two new models and improved prediction of adverse pressure gradient flows. Wang and Mujumdar (2005) applied the Yap correction (Yap, 1987) to five versions of LRN *k–ε* models for the prediction of flow characteristics of a two-dimensional turbulent slot jet. The predicted results in both stagnation and wall jet regions are in good agreement with the experimental data. Jia et al. (2007) integrated the reformulated SSG model (Spezial et al.,1991) based on the *ω*–equation and the SST model (Menter, 1994). The new model was called 'SSG-SST model'. Three cases (fully developed channel flow, backward facing step flow and impinging jet) were presented to show the performance of this model. The obtained result was better than the previous one because the new model had good applicability for complex flow fields.

The current work presents a new-concept turbulence model, namely Baseline-Low-Reynolds-Number *k–ω* with Length scale correction term (BSL-LRN *k–ω* with LSC model, BLL model). The developed model is expected to produce more accurate results for separated and reattached flows. The concept of the new model is based on a combination of accurate formulation of the Wilcox LRN *k–ω* model, LSC term in the near-wall region and concept of Baseline model. The developed model is validated with available experimental data, DNS data and numerical results using other turbulence models.

MATHEMATIC FORMULATIONS

Governing equations

The Reynolds-averaging principle is applied to the Navier-Stokes equations. After performing the averaging, the continuity and momentum equations can be shown as follows:

$$\frac{\partial \rho}{\partial t} + \frac{\partial (\rho \bar{u}_i)}{\partial x_i} = 0, \quad (1)$$

$$\frac{\partial (\rho \bar{u}_i)}{\partial t} + \frac{\partial (\rho \bar{u}_i \bar{u}_j)}{\partial x_j} = -\frac{\partial \bar{p}}{\partial x_i} + \frac{\partial \bar{\sigma}_{ij}}{\partial x_j} - \frac{\partial \left(\rho \overline{u_i' u_j'}\right)}{\partial x_j}, \quad (2)$$

where $\rho \overline{u_i' u_j'}$ are the Reynolds stresses ($R_{ij} = \rho \overline{u_i' u_j'}$).

Turbulence models

In the present work, a new model called BLL model which is based on LRN *k–ω* with LSC and transformed *k–ε*, is proposed. The standard *k–ε* model (Launder and Spalding, 1992), LRN *k–ε* model (Abe et al., 1994), High-Re *k–ω* model (Wilcox, 1993) and LRN *k–ω* model (Wilcox, 1994) are employed for results comparison.

Standard *k–ε* model: By using the Boussinesq approximation, the turbulent kinetic energy and its dissipation rate equations can be written as follows:

$$\frac{\partial (\rho k)}{\partial t} + \frac{\partial (\rho \bar{u}_j k)}{\partial x_j} = \frac{\partial}{\partial x_j}\left(\frac{\mu_t}{\sigma_k}\frac{\partial k}{\partial x_j}\right) + P_k - \rho\varepsilon, \quad (3)$$

$$\frac{\partial (\rho \varepsilon)}{\partial t} + \frac{\partial (\rho \bar{u}_j \varepsilon)}{\partial x_j} = \frac{\partial}{\partial x_j}\left(\frac{\mu_t}{\sigma_\varepsilon}\frac{\partial \varepsilon}{\partial x_j}\right) + \frac{\varepsilon}{k}(C_{\varepsilon 1} P_k - C_{\varepsilon 2}\rho\varepsilon), \quad (4)$$

where $\mu_t = \rho C_\mu k^2/\varepsilon$ is the turbulent viscosity and P_k is the production of the turbulent energy. For incompressible flow, P_k is written

as $P_k = -\rho \overline{u_i' u'}_j \dfrac{\partial \bar{u}_i}{\partial x_j} = \mu_t \left(\dfrac{\partial \bar{u}_i}{\partial x_j} + \dfrac{\partial \bar{u}_j}{\partial u_i}\right)\dfrac{\partial \bar{u}_i}{\partial x_j}$.

The model constants are given by:

C_μ = 0.09, σ_k = 1.0, σ_ε =1.3, $C_{\varepsilon 1}$ = 1.44 and $C_{\varepsilon 2}$ = 1.92.

LRN *k–ω* model: Wilcox (1994) used the near-wall concept to develop the LRN *k–ω* model. This model can be expected to show improved results for recirculating flow problems. The turbulent kinetic energy and its specific dissipation rate equations with the damping functions are shown as follows:

$$\frac{\partial (\rho k)}{\partial t} + \frac{\partial (\rho \bar{u}_j k)}{\partial x_j} = P_k - c_k f_k \rho \omega k + \frac{\partial}{\partial x_j}\left[\left(\mu + \frac{\mu_t}{\sigma_k}\right)\frac{\partial k}{\partial x_j}\right], \quad (5)$$

$$\frac{\partial (\rho \omega)}{\partial t} + \frac{\partial (\rho \bar{u}_j \omega)}{\partial x_j} = c_{\omega 1} f_\omega \frac{\omega}{k} P_k - c_{\omega 2}\rho\omega^2 + \frac{\partial}{\partial x_j}\left[\left(\mu + \frac{\mu_t}{\sigma_\omega}\right)\frac{\partial \omega}{\partial x_j}\right], \quad (6)$$

Where; μ_t is the eddy viscosity ($\mu_t = C_\mu f_\mu \rho k/\omega$) and the basic constants and the damping functions for the LRN *k–ω* model are given as follows:

$C_\mu = 1.0$, $c_k = 0.09$, $c_{\omega 1} = 0.56$, $c_{\omega 2} = 0.075$,

$\sigma_\omega = 2.0$, $\sigma_k = 2.0$,

$f_\mu = (0.025 + \mathrm{Re}_T/6)(1 + \mathrm{Re}_T/6)^{-1}$,

$f_k = \left[0.287 + (\mathrm{Re}_T/8)^4\right]\left[1 + (\mathrm{Re}_T/8)^4\right]^{-1}$,

$f_\omega = (0.1 + \mathrm{Re}_T/2.7)\left[(1 + \mathrm{Re}_T/2.7) f_\mu\right]^{-1}$, where; Re_T is the turbulent Reynolds number ($\mathrm{Re}_T = \rho k / \omega\mu$).

The BLL model: The basic idea of the new model is based on a combination of an accurate formulation of the Wilcox LRN *k–ω* model and the concept of a Baseline model to reduce the sensivity to the freestream (in the outer part of the boundary-layer and in free-shear flows). In the near-wall region, the Length Scale Correction (LSC) term is employed. The equations of the proposed model are reformulated by multiplying the LRN *k–ω* model with LSC term (Equations 7 and 8) by a function (1–F_b) and adding with the multiplication of the transformed High-Re *k–ε* equation (Eqs. (9) and (10)) and a function F_b. F_b is a blending function (a simple exponential function is used at the beginning) which ensures that the model behaves as a High-Re model away from the surface and as the LRN model in the near-wall region. For the dissipation rate equation (Equation 10), the cross diffusion term is removed. To compensate for the inferior performance of the transformed *k–ε* , the LSC term (S_ω) is employed. LRN *k–ω* model with LSC term

$$\frac{\partial(\rho k)}{\partial t}+\frac{\partial(\rho \bar{u}_j k)}{\partial x_j} = P_k - \beta^* f_{k1}\rho\omega k + \frac{\partial}{\partial x_j}\left[(\mu+\mu_t\sigma_{k1})\frac{\partial k}{\partial x_j}\right], \quad (7)$$

$$\frac{\partial(\rho \omega)}{\partial t}+\frac{\partial(\rho \bar{u}_j \omega)}{\partial x_j} = \gamma_1 f_{\omega 1}\frac{\omega}{k}P_k - \beta_1\rho\omega^2 + \frac{\partial}{\partial x_j}\left[(\mu+\mu_t\sigma_{\omega 1})\frac{\partial \omega}{\partial x_j}\right] - \rho S_\omega . \quad (8)$$

Transformed *k–ε* model (Jones and Launder, 1973)

$$\frac{\partial(\rho k)}{\partial t}+\frac{\partial(\rho \bar{u}_j k)}{\partial x_j} = P_k - \beta^* f_{k2}\rho\omega k + \frac{\partial}{\partial x_j}\left[(\mu+\mu_t\sigma_{k2})\frac{\partial k}{\partial x_j}\right], \quad (9)$$

$$\frac{\partial(\rho \omega)}{\partial t}+\frac{\partial(\rho \bar{u}_j \omega)}{\partial x_j} = \gamma_2 f_{\omega 2}\frac{\omega}{k}P_k - \beta_2\rho\omega^2 + \frac{\partial}{\partial x_j}\left[(\mu+\mu_t\sigma_{\omega 2})\frac{\partial \omega}{\partial x_j}\right]. \quad (10)$$

After rearrangement, the new model can be shown as follows:

$$\frac{\partial(\rho k)}{\partial t}+\frac{\partial(\rho \bar{u}_j k)}{\partial x_j} = P_k - \beta^* f_k\rho\omega k + \frac{\partial}{\partial x_j}\left[(\mu+\mu_t\sigma_k)\frac{\partial k}{\partial x_j}\right], \quad (11)$$

$$\frac{\partial(\rho \omega)}{\partial t}+\frac{\partial(\rho \bar{u}_j \omega)}{\partial x_j} = \gamma f_\omega\frac{\omega}{k}P_k - \beta\rho\omega^2 + \frac{\partial}{\partial x_j}\left[(\mu+\mu_t\sigma_\omega)\frac{\partial \omega}{\partial x_j}\right] - S_\omega\rho(1-F_b), \quad (12)$$

Where; $\mu_t = \rho f_\mu k/\omega$ is the turbulent viscosity and P_k is the production of the turbulent energy which can be expressed as:

$$P_k = \mu_t\left(\frac{\partial \bar{u}_i}{\partial x_j}+\frac{\partial \bar{u}_j}{\partial u_i}\right)\frac{\partial \bar{u}_i}{\partial x_j} .$$

The model constant is blended by the relation of the model constants in the LRN *k–ω* model and the transformed *k–ε* model. If ϕ_1 represent constants in the LRN *k–ω* model ($\sigma_{k1}, f_{k1}, ...$), ϕ_2 represent constants in the transformed *k–ε* ($\sigma_{k2}, f_{k2}, ...$) and ϕ represent the corresponding constants of the new model ($\sigma_k, f_k, ...$), the ϕ relation can be written as:

$$\phi = (1-F_b)\phi_1 + F_b\phi_2 . \quad (13)$$

Two sets of model constants are given as follows:

Set 1 (LRN *k–ω*) (Wilcox, 1994)

$\beta^* = 0.09$, $f_{k1} = \left[0.278 + (\mathrm{Re}_T/8)^4\right]\left[1+(\mathrm{Re}_T/8)^4\right]^{-1}$,
$\sigma_{k1} = 0.5$ $\gamma_1 = 0.56$,
$f_{\omega 1} = (0.1 + \mathrm{Re}_T/2.7)\left[(1+\mathrm{Re}_T/2.7)f_\mu\right]^{-1}$,
$\beta_1 = 0.075$, $\sigma_{\omega 1} = 2.0$ and
$f_\mu = (0.025 + \mathrm{Re}_T/6)(1+\mathrm{Re}_T/6)^{-1}$.

Set 2 (High *k–ε*) (Jones and Launder, 1973)

$\beta^* = 0.09$, $f_{k2} = 1.0$,
$\sigma_{k2} = 1.0$, $\gamma_2 = 0.44$, $f_{\omega 2} = 1.0$,
$\beta_2 = 0.0828$ and $\sigma_{\omega 2} = 0.856$.

The blending function (F_b) is selected to ensure asymptotic consistency with the near-wall behavior of the equation of motion. The value of function F_b will be designed to be zero in the near-wall region (activating the LRN model) and set to unity away from the surface (switching to the High-Re model) as shown in Figure 1. For the present model, the blending function from the LRN two-equation model of Abe et al. (1994) has been tentatively adopted, as expressed in Equation 14:

$$F_b = \left(1 - e^{-(y^*/14)}\right)^2\left(1 + 5\mathrm{Re}_T^{-0.75}\, e^{-(\mathrm{Re}_T/200)^2}\right), \quad (14)$$

Where; $y^* = (\nu\omega k)^{0.25}\, y/\nu$ and $\mathrm{Re}_T = \rho k/\omega\mu$.

Length scale correction term (LSC term)

The LSC term has been well known for turbulent separated flows. Launder (1993) applied the Yap correction (Yap, 1987) as an extra term to the *ε*–equation of LRN *k–ε* model. The Yap correction can be written as the ratio of the computational length scale to the local equilibrium length scale as follows:

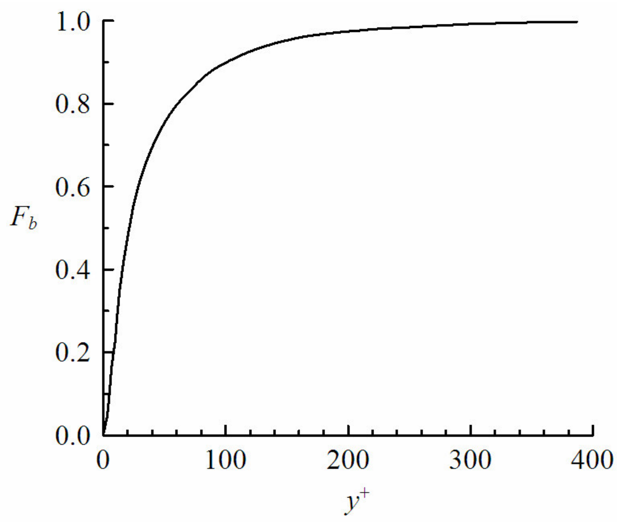

Figure 1. Blending function F_b versus y^+.

$$\rho S_\varepsilon = 0.83\rho \frac{\varepsilon^2}{k}\left(\frac{k^{3/2}}{\varepsilon \ell_e} - 1\right)\left(\frac{k^{3/2}}{\varepsilon \ell_e}\right)^2, \quad (15)$$

where ℓ_e is the local equilibrium length scale ($\ell_e = \kappa y_n / C_\mu^{3/4}$) and y_n is the normal distance to the nearest wall.

Wilcox (1993) has shown that an extra cross-diffusion term appears in the resultant ε–equation. This term, similar to the so-called "Yap correction", helps suppressing the rate of the near-wall turbulent length scale. In the present work, the turbulent length scale ($L_t = k^{1/2}/0.09\omega$) is applied to the Yap correction concept. A new length scale correction for ω–equation (LSC–ω) can be expressed as follows:

$$\rho S_\omega = 0.075 \frac{\rho k^{3/2}\omega}{\ell_e}\left(\frac{L_t}{\ell_e} - 1\right)\left(\frac{L_t}{\ell_e}\right), \quad (16)$$

Where; ℓ_ε is the near-wall equilibrium length scale ($\ell_e = C y_n$), y_n is the distance from the wall, the turbulence scale constant (C) is equal to $\kappa / C_\mu^{0.75} = 2.495$, and κ is the von Kárman constant.

NUMERICAL PROCEDURES

The finite volume method (FVM) is used to solve the set of governing equations on a staggered grid. To obtain the solution that couples the pressure and velocity, the SIMPLE algorithm (Patankar, 1980) is employed to calculate the pressure correction terms. Then, the resulting algebraic equations are iteratively solved with a line-by-line TDMA procedure. The convection terms are approximated by the second-order upwind scheme. The hybrid differencing scheme is employed in the turbulence-transport equations to ensure a stable solution procedure. The convergence criterion utilized in this work is that the maximum normalized sum of the absolute residual source for all the computed nodes is less than 10^{-6}. For all the investigated cases, the number of sufficiently small grids is ensured from the grid-independency tests.

The inlet boundary values are prescribed for all variables. At the outlet, the streamwise gradients of the flow variables are set to zero. The wall boundary conditions are applied: $u = v = 0$ and $k = 0$. The use of LRN models requires a fine grid to minimize the dependence of the solution on the grid. The boundary condition of ω at the first grid point in the near-wall region is given as (Wilcox, 1994):

$$\omega = \frac{6\nu}{c_{\omega 2} y_1^2} \quad \text{as } y_1 \to 0. \quad (17)$$

RESULTS

The present test cases are selected on the important criterion that the near-wall and low-Reynolds number effects need to be solved. Evidence of acceptable agreement with the available experimental or DNS data are expected. In the present work, calculations have been performed for the following test cases; 1) Fully developed channel flow by Moser et al. (1999), 2) Flow past backward-facing step by Jovic et al. (1994) and 3) Flow over repeated square ribs by Drain and Martin (1985).

Fully developed channel flow

The results are compared with the existing DNS data (Re_τ = 395) (Moser et al., 1999) and the predictions obtained with other models, including the results of Abe-Kordoh-Nagano LRN k–ε model (AKN (Abe et al., 1994) and Wilcox's High-Re k–ω model (Wilcox, 1993). The distributions of normalized streamwise velocity and turbulent kinetic energy compared with DNS data and other numerical results are shown in Figures 2 and 3 respectively.

For the normalized mean velocity, the proposed model and AKN model show reasonable agreement with the DNS data, whereas the Wilcox model (High-Re k–ω), with extended-to-wall method, produces noticeable underprediction in the region of $10 < y^+ < 100$.

The turbulent kinetic energy profiles ($k^+ = k/u_\tau^2$) are

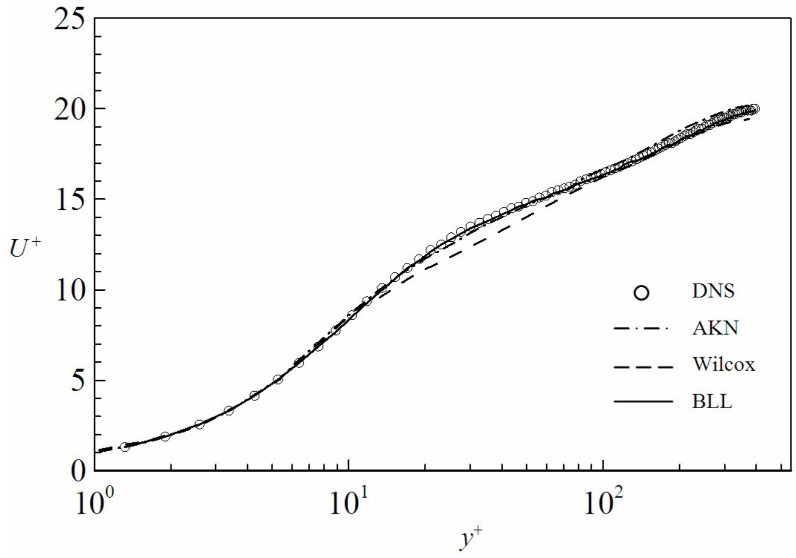

Figure 2. Normalized stream velocity profiles in near-wall region (Re_τ = 395).

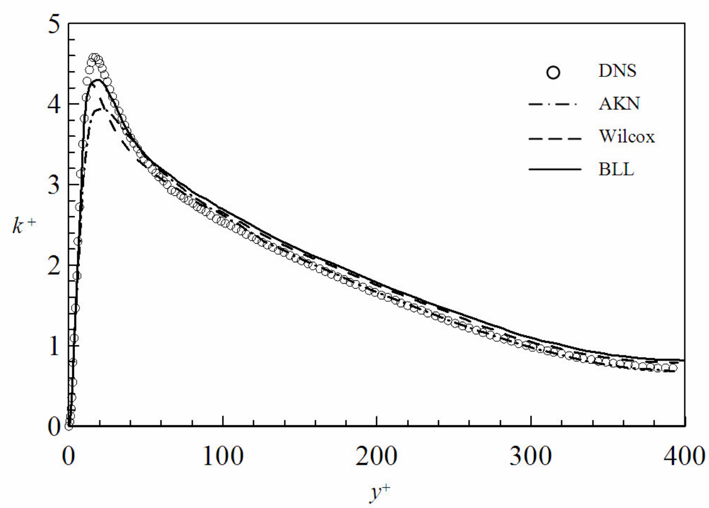

Figure 3. Turbulent kinetic energy profiles in near-wall region (Re_τ = 395).

shown in Figure 3. It can be seen that the results from all models are in good agreement with the DNS data especially for $y^+ > 30$. The proposed model gives better results than other models at peak interval.

Flow past backward-facing step (BFS)

The backward-facing step flow demonstrates complex flow phenomena including redeveloping boundary layers such as recirculation, separation and reattachment. It is typically considered as a suitable test case for turbulence model validation.

The ability of the proposed model is shown through simulations for double-sided BFS flows at Re_h = 5,000. The backward-facing step configuration is symmetric about the centerline of the channel. Thus, only half of the channel is employed as the computational domain (Figure 4). The fully-developed flow profile at the inlet is set according to the experimental data of Jovic et al. (1994).

Figure 4 illustrates the geometry of the backward-facing-step domain (a symmetrically sudden double-sided expansion). Following the experimental data of Jovic et al. (1994), interest in this flow with the DNS method was revived by Le et al. (1997) The step height (h) on each

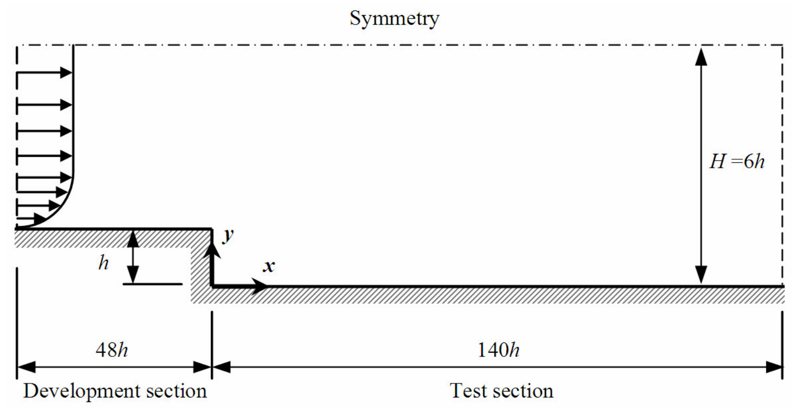

Figure 4. Backward facing step configuration.

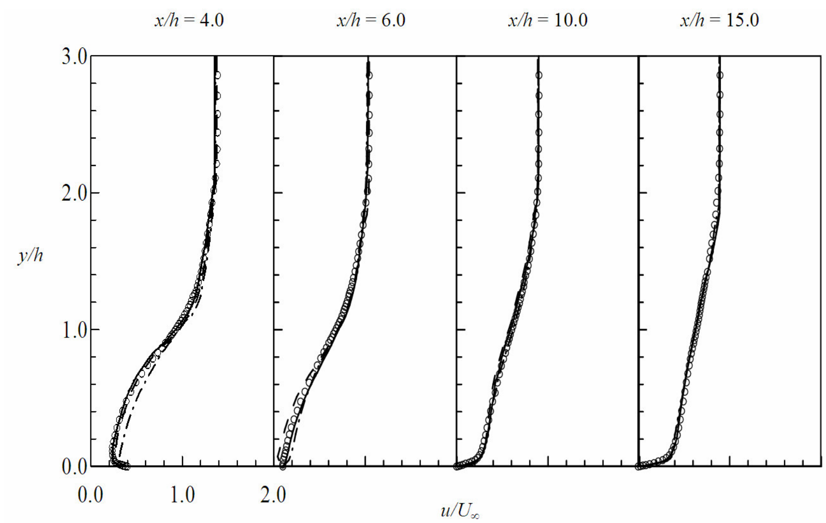

Figure 5. Normalized mean stream wise velocities (u/U_∞) for BFS flow,

○ DNS data, –·– AKN model, – – – Wilcox model, —— BLL model .

side is 9.6 mm. The test section length is 12*h*. The Reynolds number based on the reference flow velocity and step height $(\mathrm{Re}_h = U_\infty h/\nu)$ is 5,000.

Figure 5 shows model comparisons of the mean streamwise velocity (normalized by the reference flow velocity (u/U_∞)) at the locations *x/h* = 4.0, 6.0, 10.0 and 15.0, respectively – *x* = 0.0 is the location of the sudden expansion.

The obtained results can be divided into two regions. In the recirculation region, $0.0 \le x/h \le 6.0$, the proposed model presents obviously improved prediction compared with those of other turbulence models. In the redeveloping region, $x/h \ge 10.0$, all models give fair consistency with DNS data. The reattachment length parameter (X_r) is employed to designate the improved performance of the turbulence model. The dimensionless reattachment length of the primary recirculation (X_r/h) from DNS data is 6.28 and the results from AKN, Wilcox and the proposed models are, X_r/h = 5.7, 7.8 and 6.8, respectively.

Figure 6 illustrates the normalized turbulent kinetic energy profiles (k/U_∞^2) at different locations. Better prediction can obviously be seen here. In the recirculation region (at X_r/h = 4.0 and 6.0), all models underpredict the turbulence level. The low level of turbulence implies that the recirculation size is large (the proposed model and Wilcox model).

The skin friction coefficient distribution ($C_f = 2\tau_w(\rho U_\infty^2)$) is shown in Figure 7. The coefficient in the redeveloping zone $(x/h \ge 10.0)$ presents some dis-crepancies. The overestimated C_f may arise from high level of recovery

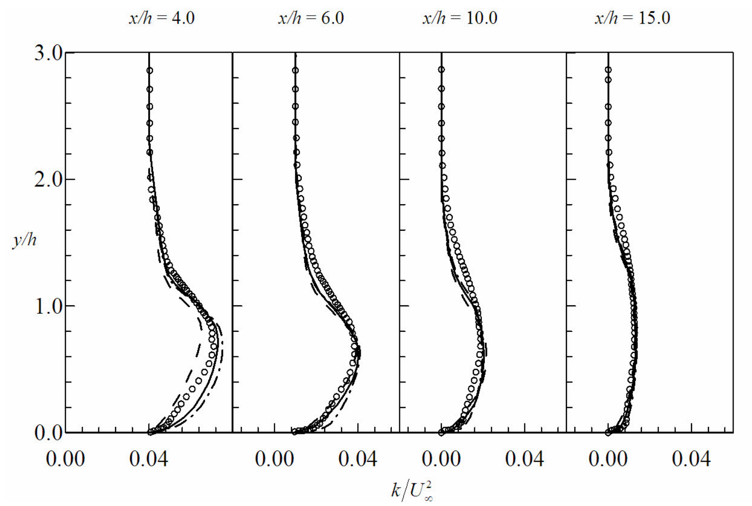

Figure 6. Turbulent kinetic energy $\left(k/U_{\infty}^{2}\right)$ for BFS flow,

○ DNS data, –·– AKN model, – – – Wilcox model, —— BLL model .

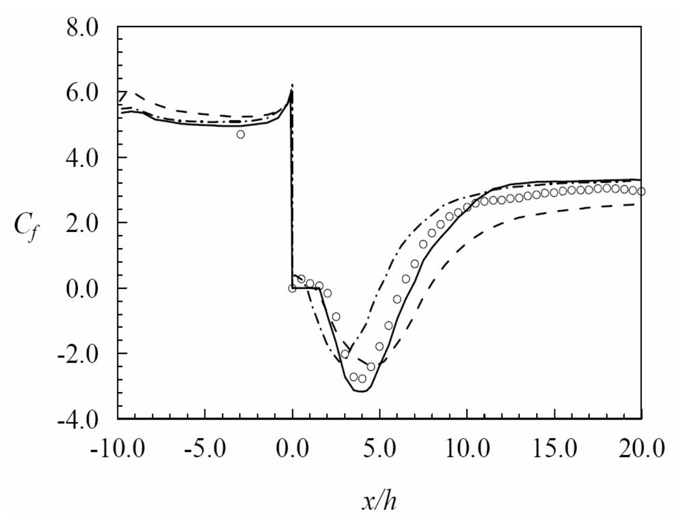

Figure 7. Skin friction coefficients for BFS flow,

○ DNS data, –·– AKN model, – – – Wilcox model, —— BLL model

of the developed turbulent flow in this area.

Flow over repeated square ribs

The final test case is the flow over repeated square ribs. Cui et al. (2003) used Large Eddy Simulation (LES) to study the flow in a two-dimensional channel with ribs, and investigated the results of various pitch-to-height ratios. Repeated studies were indicated by Miyake et al. (2002), Ikeda and Durbin (2002) (using DNS) and Ryu et al. (2007) (using the LRN k–ω model).

For the unity aspect ratio (channel height-to-width ratio), the side-wall effects can be neglected and the flow is considered to be a 2-D simulation. The report of Ooi et al. (1998, 2000) confirms that the numerical method produce accurate results. The experimental data from Drain and Martin (1985) are used for validating flow over a smooth wall with square sectioned ribs (experimental data available on URL shown in Drain and Martin (1985)). The spanwise square ribs are mounted on the bottom wall of a channel as shown in Figure 8. The Reynolds number (Re_{De} = 37,200) is calculated with respect to the bulk velocity (U_b) and the hydraulic diameter (De). A 2-D Cartesian grid is employed, as shown in Figure 9. To solve the near-wall flow problem, fine-grid spacing is applied in the region next to the channel walls and rib surfaces.

Dimensions of the test case are given as follows: the

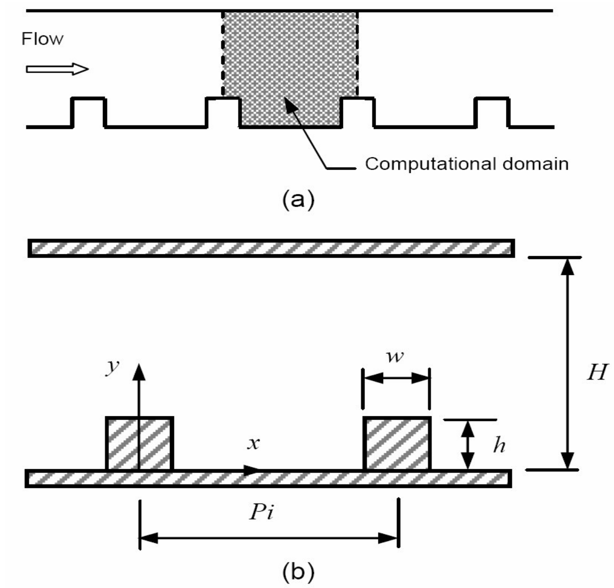

Figure 8. (a) Computational domain (b) Repeated square ribs configuration.

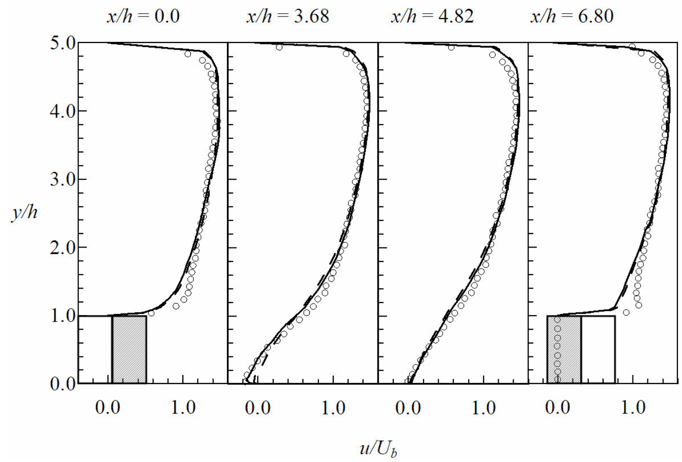

Figure 10. Normalized mean streamwise velocities (u/U_b) for flow over repeated square ribs,

○ Experimental data, - - - High-Re k–ε model, —— BLL model

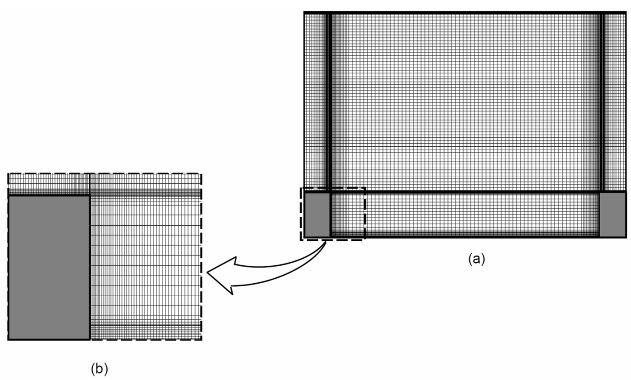

Figure 9. (a) Computational domain (b) Repeated square ribs configuration.

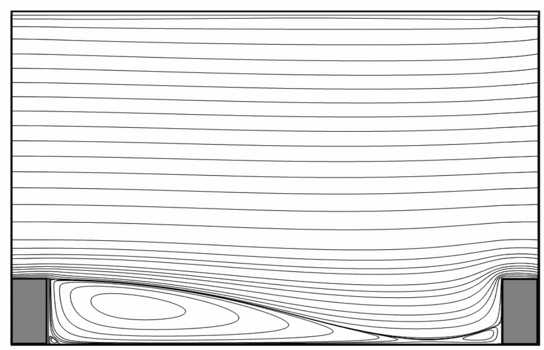

Figure 11. Predicted Streamlines from BLL model (ribbed-channel flow at Re_{De} = 37,200).

size of each rib is 8 × 8 mm, the pitch-to-height ratio (*Pi/h*) is 7.2 and the channel-to-rib height ratio (*H/h*) is 5.0. The inlet and outlet sections are prescribed with periodic boundary conditions.

The normalized streamwise velocity profiles at different locations *(x/h* = 0.0, 3.68, 4.82 and 6.80) are presented in Figure 10. It can be seen that the numerical results are in satisfactory agreement with the experimental data of Drain and Martin (1985) in all region. Some discrepancies are found in the region above rib surfaces. Manceau et al. (2000) in noting these types of discrepancies, suggested that the experiment probably exhibited 3-D effects such as counter rotating eddies in the *x*-direction located between the top surface of the ribs and the upper channel wall. These effects might induce flow acceleration on the measurement plane where they converge and deceleration where they diverge.

In the region between two ribs, two recirculation zones can be observed. These recirculation regions may be merged as illustrated in Figure 11. The experiment reports the reattachment of the ribbed channel flow at about 4.32 *h*, whereas the proposed model gives the value of approximately 4.59 *h*. Thus, the present simulations with the BLL turbulence model indicate a 6.3 % overprediction of the reattachment length compared to the experimental result. For High-Re model results, the small separated bubbles were observed (not shown here).

The normalized turbulent shear stress profiles $(-\overline{uv}/U_b^2)$ at various locations are plotted as shown in Figure 12. The predicted profiles at the location, *x/h* = 3.68 and 4.82 are in good agreement. However, at *x/h* = 6.80 (rib-top region), the turbulent shear stresses given by all models are quit different from the experimental results. This discrepancy may be attributed to the 3-D

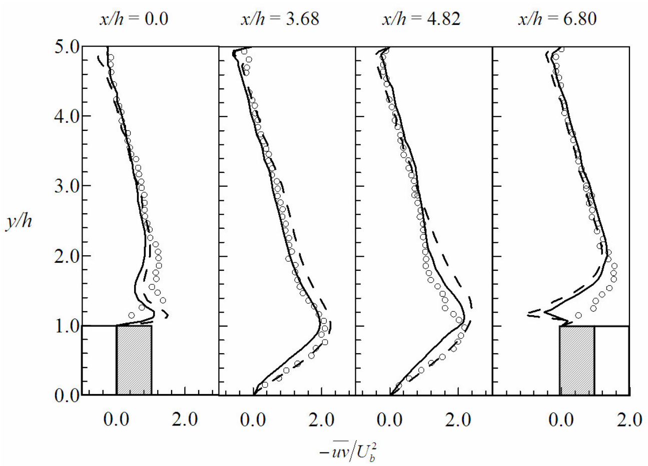

Figure 12. Normalized turbulent shear stress $\left(-\overline{uv}/U_b^2\right)$ for flow over repeated square ribs,
○ Experimental data, – – – High-Re k–ε model, —— BLL model .

effects as found in the case of the velocity distribution (Figure 10).

Conclusions

In this study, a new-concept turbulence model for recirculating flows is presented. The proposed model combines new LSC term, ω–LSC term, using an analogy to the Yap correction to correct the result in the near-wall region, and the concept of a Baseline model to reduce the sensivity to the freestream. Performance of the model is validated by three well-known test cases: fully developed channel flow, BFS flow, and flow over repeated square ribs. The results are satisfactory for all test cases. The prediction reproduces the correct wall-limiting behaviors of the flow field. However, discrepancies exist in some cases (BFS flow and flow in ribbed channel) because of the 3-D effects such as counter-rotating eddies in the *x*-direction located between the top surface of the ribs and upper channel wall.

The combined low-Reynolds number k–ω model and the new LSC term have demonstrated their performance for accommodating the near-wall low-Reynolds number effect for turbulent recirculating flows. Examples of three flows may be found in combustors, heat exchangers, electronic circuit cooling systems and complex geometrical features of the cooling passages in gas turbine blades.

ACKNOWLEDGEMENTS

This work was supported by the Research Grant for New Scholar (RGNS) from the Commission on Higher Education and Thailand Research Fund (TRF) with Prof. P. Dechaumphai as the project mentor.

REFERENCES

Abe K, Kondoh T, Nagano Y (1994). A new turbulence model for predicting fluid flow and heat transfer in separating and reattaching flows - I. Flow field calculations. Int. J. Heat Mass Tran. 37: 139-151.

Abid R (1993). Evaluation of two-equation turbulence models for predicting transitional flows. Int. J. Eng. Sci. 31: 831–840.

Chang KC, Hsieh WD, Chen CS (1995). A modified low-Reynolds-number turbulence model applicable to recirculating flow in pipe expansion. J. Fluid Eng-T. ASME 117: 417-423.

Chien KY (1982). Predictions of channel and boundary-layer flows with a low-Reynolds-number turbulence model. AIAA J. 20: 33-38.

Cui J, Patel VC, Lin CL (2003). Large-eddy simulation of turbulent flow in a channel with rib roughness. Int. J. Heat Fluid Fl. 24: 372-388.

Drain LE, Martin S (1985). Two-component velocity measurements of turbulent flow in a ribbed-wall flow channel. International Conference on Laser Anemometry – Advances and Applications. UK.

Ikeda T, Durbin PA (2002). Direct simulations of a rough-wall channel flow. Mechanical engineering Report TF-81. Stanford University. UK.

Jia R, Sunden B, Faghri M (2007). A new low Reynolds stress transport model for heat transfer and fluid in engineering applications. J. Heat Trans-T. ASME 129: 434-440.

Jones WP, Launder BE (1973). The calculation of low-Reynolds-number phenomena with a two-equation model of turbulence. Int. J. Heat Mass Tran. 16: 1119-1130.

Jovic S, Alto P, Driver DM (1994). Backward-facing step measurements at low Reynolds number, Reh = 5000. NASA TM-108807. NASA-Ames research center. USA: 1-24. http://tmdb.ws.tn.tudelft.nl/workshop7/case7_2/case72d.html.

Lam CK, Bremhorst K (1981). A modified form of the k–♏ model for predicting wall turbulence. J. Fluid Eng-T. ASME 103: 456-460.

Larsson J (1999). Numerical Simulation of Turbulent Flows for Turbine Blade Heat Transfer Applications. Ph.D. Dissertation. Chalmers University of Technology.

Launder BE (1993). Modelling convective heat transfer in complex turbulent flows. Proceedings of the Second International Symposium - Engineering Turbulence Modeling and Experiments 2. Elsevier press. Italy.

Launder BE, Spalding DB (1972). Mathematical Models of Turbulence. Academic Press, London.

Launder BE and Spalding DB (1990). The numerical computation of turbulent flows. Comput. Method Appl. M. 3: 269-289.

Le H, Moin P, Kim J (1997). Direct numerical simulation of turbulent flow over a backward-facing step. J. Fluid Mech. 330: 349-374.

Manceau R, Parneix S, Laurence D (2000). Turbulent heat transfer predictions using the model on unstructured mesh. Int. J. Heat Fluid Fl. 21: 320-328.

Menter FR (1992). Improved two-equation k–ω turbulence models for aerodynamic flows. NASA TM-103975. NASA-Ames research center. USA: 1-31.

Menter FR (1994). Two-equation eddy-viscosity turbulence models for engineering applications. AIAA J. 32: 1598-1605.

Miyake Y, Tsujimoto K, Nagai N (2002). Numerical simulation of channel flow with a rib-roughened wall. J. Turbul. 3: 1-17.

Moser RD, Kim J, Monsour NN (1999). Direct numerical simulation of the turbulent channel flow up to Reτ= 590. Phys. Fluids. 11: 943-945.

Ooi A, Iaccarino B, Behnai M (1998). Heat transfer predictions in cavities (in CTR summer program). Center for Turbulence Research. Stanford University. UK.

Ooi A, Reif BP, Iaccarino B, Durbin P (2000). Evaluation of RANS for rotating flows (in CTR summer program). Center for Turbulence Research. Stanford University. UK.

Patankar SV (1980). Numerical Heat Transfer and Fluid Flow. McGraw-Hill, Washington. USA.

Patel VC, Rodi W, Scheuerer G (1985). Turbulence models for near-wall and low Reynolds numbers flows – A review. AIAA J. 23: 1308-1319.

Patel VC, Yoon JY (1995). Application of turbulence models to separated flow over rough surfaces. J. Fluid Eng-T. ASME 117: 234-241.

Peng SH, Davidson L, Holmberg S (1997). A modified low-Reynolds-number k–ω model for recirculating flows. J. Fluid Eng-T. ASME 119: 867-875.

Peng SH, Davidson L (1999). Computation of turbulent buoyant flows in enclosures with low-Reynolds-number k–ω models. Int. J. Heat Fluid Fl. 20: 172-184.

Ryu DN, Choi DH, Patel VC (2007). Analysis of turbulent flow in channels roughened by two-dimensional ribs and three-dimensional blocks, Part I : Resistance. Int. J. Heat Fluid Fl. 28: 1098-1111.

Speziale CG, Abid R, Anderson EC (1992). Critical evaluation of two-equation models for near-wall turbulence. AIAA J. 30: 324-325.

Spezial CG, Sarkar S, Gatski TB (1991). Modelling the pressure-strain correlation of turbulence: an invariant dynamical systems approach. J. Fluid. Mech. 227: 245-272.

Wang SJ, Mujumdar AS (2005). A comparative study of five low Reynolds number k–ɱ models for impingement heat transfer. Appl. Therm. Eng. 25 :31-44.

Wilcox DC (1988). Multiscale model for turbulent flows. AIAA J. 26: 1311-1320.

Wilcox DC (1993). Turbulence Modeling for CFD. DCW Industries Inc., California. USA.

Wilcox DC (1994). Simulation of transition with a two-equation turbulence model. AIAA J. 33: 247-255.

Yap CJ (1987). Turbulent Heat and Momentum Transfer in Recirculating and Impinging Flows. Ph.D. Dissertation. University of Manchester.